TWMS J. App. and Eng. Math. V.15, N.3, 2025, pp. 526-537

CUBIC-BSPLINE COLLOCATION METHOD FOR NUMERICAL SOLUTIONS OF THE NONLINEAR FRACTIONAL ORDER KLEIN–GORDON EQUATION

J. DAMIRCHI[1*], S. SHAGHOLI[2], S. FOADIAN[3], §

Abstract. This research paper focuses on utilizing the cubic-Bspline collocation method to obtain numerical solutions for the time-fractional nonlinear Klein–Gordon (TFNKG) equation. The Klein–Gordon (KG) equation, which characterizes nonlinear wave propagation, is extended by replacing the time derivative in Caputo sense of order derivative of order α, $(1 < \alpha \leq 2)$. The **L2** discretization formula is employed to approximate the time-fractional derivative. The spatial variable is discretized using cubic B-spline basis functions, and the nonlinear terms are linearized using the quasilinearization technique. Through the proposed method, the main problem is transformed into a more computationally manageable problem. Numerical examples involving different types of nonlinearities are tested to demonstrate the accuracy of the developed scheme. The simulations confirm the high accuracy of the proposed method when compared to analytical solutions, as well as other methods such as the Sinc-Chebyshev collocation method (SCCM) and the variational iteration method (VIM). The accuracy of the developed scheme is also evaluated using error norms L_∞ and L_2. The research findings of this study substantiate the efficacy and credibility of the proposed methodologies in the analysis of fractional differential equations.

Keywords: Fractional Klein–Gordon equation, Caputo derivative, Cubic-Bspline method, Quasilinearization.

AMS Subject Classification: 65Nxx, 74G15, 35R11

1. Introduction

Fractional-order calculus has received considerable attention in the engineering and physical sciences over the last few decades to model several diverse phenomena in robotic technology, bio-engineering, control theory, viscoelasticity diffusion model, relaxation processes, and signal processing [1,22]. The order of derivatives, as well as integrals in the

[1,2] Faculty of Mathematics, Statistics and Computer Science, Semnan University, Semnan, Iran.
e-mail: damirchi@semnan.ac.ir; https://orcid.org/0000-0002-4878-1921.
e-mail: sshagholi@semnan.ac.ir; https://orcid.org/0000-0002-4538-8892.
[3] School of Mathematics and Computer Science, Damghan University, Damghan, Iran.
e-mail: s.foadian@std.du.ac.ir; https://orcid.org/0000-0001-7091-1254.
[*] Corresponding author.
§ Manuscript received: September 2, 2023; accepted: January 11, 2024.
TWMS Journal of Applied and Engineering Mathematics, Vol.15, No.3;

fractional-order calculus, is arbitrary. Therefore, fractional-order nonlinear partial differential equations (NPDEs) have developed a fundamental interest in generalizing integer-order NPDEs to model complex systems in thermodynamics, engineering, fluid dynamics, and optical physics [16]. Many considerable works on the theoretical analysis [5,32] have been carried on. In the field of solving applied problems, there are several fractional differential equations that have extensive applications in physics and engineering. Some of these equations include: the fractional Hamiltonian amplitude equation, fractal-fractional shallow water wave equation, fractional modified Kdv–Kadomtsev–Petviashvili equation, the local fractional Bogoyavlensky–Konopelchenko model, the fractional Kdv–Zakharov–Kuznetsov equation, and the modified fractal gas dynamics model [26–31].

There are several definitions of a fractional derivative of order $\alpha > 0$ [20]. The two most commonly used are the Riemann–Liouville and Caputo. In this paper, we will use the Caputo fractional derivative which is

$$
{}_a^c D_t^\alpha \varphi(t) = \begin{cases} \frac{1}{\Gamma(n-\alpha)} \int_a^t \frac{\varphi^{(n)}(\tau)}{(t-\tau)^{\alpha+1-n}} \, d\tau, & n-1 < \alpha < n, \\ \\ \frac{d^n \varphi(t)}{dt^n}, & \alpha = n \in \mathbb{N}, \end{cases}
$$

where $\Gamma(\cdot)$ is the Gamma function.
The KG equation considered herein is a basic nonlinear evolution equation that arises in relativistic quantum mechanics. It was formulated by *Erwin Schrödinger* for the non-relativistic wave equation in quantum physics, while precisely studied by the famous physicists *Oskar Klein* and *Walter Gordon* in 1926 [10,14]. The KG equation has an extensive variety of applications in classical field theory [2] as well as in quantum field theory [3]. It has also been extensively used in numerous areas of physical phenomena such as in solid-state physics, dispersive wave phenomena, nonlinear optics, elementary particle behavior, dislocations propagation in crystals, and different classes of soliton solutions [13]. The classical KG equation, which is based on the assumption of homogeneous space and time, is inadequate for explaining chargeless systems and single-particle systems at mesoscopic and macroscopic scales. This is because, in such scales, space and time exhibit non-homogeneous behavior that cannot be accurately described using classical calculus. To address this limitation, the TFNKG equation has been proposed as an alternative. Hence, in this paper, we explore a generalized form of KG by considering a Caputo fractional time derivative of order $1 < \alpha \leq 2$, as follows:

$$
\frac{\partial^\alpha \varphi}{\partial t^\alpha} + a_0 \frac{\partial^2 \varphi}{\partial x^2} + b_0 \varphi + c_0 \varphi^\beta = G(x,t), \qquad 0 < x < 1, \ 0 < t < t_f, \tag{1}
$$

with the initial and Dirichlet boundary conditions

$$
\varphi(x,0) = f_1(x), \qquad \frac{\partial \varphi}{\partial t}(x,0) = f_2(x), \qquad 0 \leq x \leq 1, \tag{2}
$$

$$
\varphi(0,t) = p(t), \qquad \varphi(1,t) = q(t), \qquad 0 \leq t \leq t_f, \tag{3}
$$

where $\varphi = \varphi(x,t)$ represents the wave displacement at position x and time t, the parameters a_0, b_0, and c_0 are real constants, $\beta = 2$ or $\beta = 3$, $G(x,t)$ stands for the source term, and $f_1(x)$, $f_2(x)$, $p(t)$, and $q(t)$ are analytical known functions. Also, $\frac{\partial^\alpha \varphi}{\partial t^\alpha}$ is the time-fractional derivative the Caputo sense as follows

$$
\frac{\partial^\alpha \varphi(x,t)}{\partial t^\alpha} = \begin{cases} \frac{1}{\Gamma(2-\alpha)} \int_0^t \frac{1}{(t-\tau)^{\alpha-1}} \frac{\partial^2 \varphi(x,\tau)}{\partial \tau^2} \, d\tau, & 1 < \alpha < 2, \\ \\ \frac{\partial^2 \varphi(x,t)}{\partial t^2}, & \alpha = 2. \end{cases}
$$

For $\alpha = 2$, we get the classical KG equation which appears in classical relativistic and quantum mechanics and analysis of wave propagation in linear dispersive media. The fractional KG equation extends the classical KG equation. Additionally, this equation has been used to model a wide range of physical phenomena, including:

- Nonlinear waves, such as shock waves and solitary waves;
- Fractal structures, such as coastlines and snowflakes;
- Anomalous diffusion, such as diffusion in disordered media.

As we know, there is no classical method to handle the nonlinear fractional partial differential equations and provide the explicit solution due to the complexities of fractional calculus. For this reason, we need accurate semi-analytical or numerical approaches to find the approximate solution of such problems. Some authors studied the analytical and numerical methods to find the analytical or approximate solutions of fractional differential equations [9,11,12,15,21]. The fractional order KG equation is solved by the Sinc–Chebyshev collocation method in [18]. Singh et al. [24], presented a reliable numerical algorithm for the fractional KG equation. In [23], an efficient computational method is applied to solve the time-space fractional KG equation. Ganji et al., applied clique polynomials to solve the time-fractional KG equations [8]. In this regard, we apply the cubic B-spline method to obtain the numerical solution of the problem (1)–(3).

The remainder of the work is arranged in the following sections. In Section 2, the properties of the cubic B-splines collocation method are discussed. In Section 3, the application of the cubic B-spline method to get numerical solutions of the TFNKG equation is presented. The numerical computations and results are made in Section 4. Finally, concluding remarks are drawn in Section 5.

2. Cubic B-spline functions

In this Section, we describe the uniform cubic B-spline on the finite interval $[0, 1]$. For this purpose, we divide the interval $[0, 1]$ into M-subintervals by the set of $M + 1$ nodal points x_i, $0 \leq i \leq M$. This gives a partition $\pi : 0 = x_0 < x_1 < \cdots < x_{M-1} < x_M = 1$ of $[0, 1]$, where $\Delta x_i = x_i - x_{i-1}$, $\forall\ 1 \leq i \leq M$. The cubic B-splines are constructed for the partition

$$\Pi : x_{-2} < x_{-1} < x_0 = 0 < x_1 < \cdots < x_M = 1 < x_{M+1} < x_{M+2},$$

by using four fictitious nodes $x_{-2}, x_{-1}, x_{M+1}, x_{M+2}$.
If we assume that $\Delta x_i = h_x$, $\forall\ -1 \leq i \leq M + 2$, then the uniform cubic B-splines are defined by, [7],

$$B_i(x) = \frac{\Delta^4 F_x(x_{i-2})}{h_x^3},$$

where

$$F_x(x_i) = (x_i - x)_+^3 = \begin{cases} (x_i - x)^3, & x < x_i, \\ 0, & x \geq x_i, \end{cases}$$

and $\Delta^4 F_x(x_i)$ is the fourth forward difference with equally spaced nodes of third-degree polynomial $F_x(x_i)$. After some simplification, we get

$$B_i(x) = \frac{1}{h_x^3} \begin{cases} (x - x_{i-2})^3, & x_{i-2} \leq x < x_{i-1}, \\ h_x^3 + 3h_x^2(x - x_{i-1}) + 3h_x(x - x_{i-1})^2 - 3(x - x_{i-1})^3, & x_{i-1} \leq x < x_i, \\ h_x^3 + 3h_x^2(x_{i+1} - x) + 3h_x(x_{i+1} - x)^2 - 3(x_{i+1} - x)^3, & x_i \leq x < x_{i+1}, \\ (x_{i+2} - x)^3, & x_{i+1} \leq x \leq x_{i+2}, \\ 0, & \text{otherwise}. \end{cases} \tag{4}$$

It can be easily see that the functions in $\{B_{-1}, B_0, \ldots, B_M, B_{M+1}\}$ are linearly independent on $[0,1]$, ([6]). By using splines defined in (4), the values of $B_i(x)$ and its derivatives at the nodes x_i's are given in Table 1.

TABLE 1. The values of $B_i(x)$ and its derivatives at the nodal points.

	x_{i-2}	x_{i-1}	x_i	x_{i+1}	x_{i+2}
$B_i(x)$	0	1	4	1	0
$B_i'(x)$	0	$\frac{3}{h_x}$	0	$\frac{-3}{h_x}$	0
$B_i''(x)$	0	$\frac{6}{h_x^2}$	$\frac{-12}{h_x^2}$	$\frac{6}{h_x^2}$	0

3. Description of the proposed method

In this Section, we present the application of the cubic B-spline method to get numerical solutions to the problem (1)–(3).

3.1. **Space discretization by the cubic B-spline.**

In this subsection, we introduce our method based on the cubic B-spline functions for the discretization of spatial derivatives that appeared in the TFNKG equation (1). To apply the proposed method, express $\varphi(x,t)$ by using cubic B-spline functions. Let

$$\varphi(x,t_j) \cong \sum_{i=-1}^{M+1} \sigma_i^j B_i(x), \tag{5}$$

be the approximate solution of the problem (1) at the j-th time level, where σ_i^j is unknown time-dependent quantities to be determined.

Using approximate solution (5) and cubic B-spline (4), the approximate values at the knots of $\varphi(x_i,t_j)$ and its derivatives up to the second order are determined in terms of the time parameters σ_i^j as

$$\varphi(x_i,t_j) = \sigma_{i-1}^j + 4\sigma_i^j + \sigma_{i+1}^j, \tag{6}$$

$$\varphi'(x_i,t_j) = \Big(\frac{3}{h_x}\Big)\Big(\sigma_{i+1}^j - \sigma_{i-1}^j\Big), \tag{7}$$

$$\varphi''(x_i,t_j) = \Big(\frac{6}{h_x^2}\Big)\Big(\sigma_{i-1}^j - 2\sigma_i^j + \sigma_{i+1}^j\Big). \tag{8}$$

3.2. **Time discretization of the time-fractional derivative.**

Within this section, our objective is to discretize the time-fractional derivatives. We employ the **L2** formula to discretize Caputo's fractional derivative depicted in equation (1) as follows [20]:

$$\frac{\partial^\alpha \varphi}{\partial t^\alpha}(x,t_{j+1}) = \gamma_\alpha \sum_{m=0}^{j} \omega_m \Big[\varphi(x,t_{j-m+1}) - 2\varphi(x,t_{j-m}) + \varphi(x,t_{j-m-1})\Big], \tag{9}$$

where

$$\gamma_\alpha = \frac{h_t^{-\alpha}}{\Gamma(3-\alpha)}, \qquad \omega_m = (m+1)^{2-\alpha} - m^{2-\alpha},$$

where h_t is the time step. In equation (1), if we use the linearization

$$(1-\beta)\varphi^\beta(x,t_j) + \beta\varphi^{\beta-1}(x,t_j)\varphi(x,t_{j+1}),$$

which is similar to the quasilinearization technique [4], instead of nonlinear term $\varphi^\beta(x,t_{j+1})$, and set the approximation (9) in this equation, we obtain

$$\begin{aligned}&\Big[\gamma_\alpha + b_0 + c_0\beta\varphi^{\beta-1}(x,t_j)\Big]\varphi(x,t_{j+1}) + a_0\frac{\partial^2\varphi}{\partial x^2}(x,t_{j+1})\\ &= G(x,t_{j+1}) + c_0(\beta-1)\varphi^\beta(x,t_j) + \gamma_\alpha\Big[2\varphi(x,t_j) - \varphi(x,t_{j-1})\Big]\\ &- \gamma_\alpha\left[\sum_{m=1}^{j}\omega_m\Big(\varphi(x,t_{j-m+1}) - 2\varphi(x,t_{j-m}) + \varphi(x,t_{j-m-1})\Big)\right].\end{aligned} \tag{10}$$

Now, substituting the approximate values (6) and (8) in equation (10) yield the following equation with the variable σ

$$\begin{aligned}&\theta_1\sigma_{i-1}^{j+1} + \theta_2\sigma_i^{j+1} + \theta_1\sigma_{i+1}^{j+1} = G(x_i,t_{j+1}) + c_0(\beta-1)\Big[\sigma_{i-1}^j + 4\sigma_i^j + \sigma_{i+1}^j\Big]^\beta\\ &+ \gamma_\alpha\left[2\Big[\sigma_{i-1}^j + 4\sigma_i^j + \sigma_{i+1}^j\Big] - \Big[\sigma_{i-1}^{j-1} + 4\sigma_i^{j-1} + \sigma_{i+1}^{j-1}\Big]\right]\\ &-\gamma_\alpha\left[\sum_{m=1}^{j}\omega_m\left(\Big[\sigma_{i-1}^{j-m+1} + 4\sigma_i^{j-m+1} + \sigma_{i+1}^{j-m+1}\Big] - 2\Big[\sigma_{i-1}^{j-m} + 4\sigma_i^{j-m} + \sigma_{i+1}^{j-m}\Big]\right.\right.\\ &\qquad\left.\left. + \Big[\sigma_{i-1}^{j-m-1} + 4\sigma_i^{j-m-1} + \sigma_{i+1}^{j-m-1}\Big]\right)\right]\end{aligned} \tag{11}$$

where $i = 0,1,\dots,M$, $j = 0,1,\dots,$ and

$$\theta_1 = \mathcal{R} + \frac{6a_0}{h_x^2}, \qquad \theta_2 = 4\mathcal{R} - \frac{12a_0}{h_x^2}, \qquad \mathcal{R} = \gamma_\alpha + b_0 + c_0\beta\Big(\sigma_{i-1}^j + 4\sigma_i^j + \sigma_{i+1}^j\Big)^{\beta-1}.$$

System (11) consists of $(M+1)$ linear equations in $(M+3)$ unknowns $(\sigma_{-1},\sigma_0,\sigma_1,\dots,\sigma_{M+1})$. To obtain a unique solution to the resulting system two additional constraints are required. These are obtained by imposing boundary conditions (3). Eliminating σ_{-1}, and σ_{M+1} the system gets reduced to a matrix system of dimension $(M+1)\times(M+1)$ which is a tridiagonal system that can be solved by Thomas algorithm [25]. Finally, we can obtain

$$\varphi(x_i,t_j) = \sigma_{i-1}^j + 4\sigma_i^j + \sigma_{i+1}^j, \qquad i = 0,1,\dots,M, \qquad j = 1,2,\dots$$

3.3. **The initial vector.** At a particular time level, the approximate solution $\varphi(x,t)$ can be determined repeatedly by solving the recurrence relation, once the initial vectors have been computed from the initial conditions.
From the initial condition

$$\varphi(x_i,0) = f_1(x_i), \qquad i = 0,1,\dots,M,$$

we get $(M+1)$ equations in $(M+3)$ unknowns. The two unknowns σ_{-1}^0 and σ_{M+1}^0 can be obtained from the relation $\varphi_x(x_0,0) = f_1'(x_0)$ and $\varphi_x(x_M,0) = f_1'(x_M)$ at the knots. It leads to a system of $(M+1)$ equations in $(M+1)$ unknowns which can be solved by Thomas algorithm.
Also, given that $\varphi(x,t_{-1}) = f_1(x) - h_t f_2(x)$, from the initial conditions

$$\varphi(x_i,0) = f_1(x_i), \qquad \frac{\partial\varphi}{\partial t}(x_i,0) = f_2(x_i), \qquad i = 0,1,\dots,M,$$

we get $(M+1)$ equations in $(M+3)$ unknowns. The two unknowns σ_{-1}^{-1} and σ_{M+1}^{-1} can be obtained from the relation $\varphi_x(x_0,0) = f_1'(x_0)$, $\varphi_x(x_M,0) = f_1'(x_M)$, $(\frac{\partial\varphi}{\partial t})_x(x_0,0) = f_2'(x_0)$, and $(\frac{\partial\varphi}{\partial t})_x(x_M,0) = f_2'(x_M)$ at the knots. It leads to a system of $(M+1)$ equations in $(M+1)$ unknowns which can be solved by the Thomas algorithm.

4. Numerical computations and results

In this Section, numerical computations of the TFNKG equation (1) with the initial and boundary conditions (2) and (3) are obtained. To gain insight into the performance of the suggested method, two numerical examples are given in this section. The accuracy of the proposed techniques is measured in terms of error norms L_∞ and L_2 for $0 < x < 1$ and $0 < t \leq t_f$ which are defined as follows:

$$L_\infty = ||\varphi_{exact}(x,t) - \varphi_{approx}(x,t)||_\infty = \max|\varphi_{exact}(x,t) - \varphi_{approx}(x,t)|,$$

$$L_2 = \sqrt{h_x \sum_{i=1}^{M}\Big(\varphi_{exact}(x_i,t) - \varphi_{approx}(x_i,t)\Big)^2}, \quad L_2 = \sqrt{h_t \sum_{j=2}^{N+1}\Big(\varphi_{exact}(x,t_j) - \varphi_{approx}(x,t_j)\Big)^2},$$

where $h_x = \frac{1}{M}$ and $h_t = \frac{t_f}{N}$.
For the graphical analysis as well as for the computations in this paper MATLAB (R2015b) has been operated.

4.1. Test problems.

Example 4.1. *Consider the following TFNKG equation [18]:*

$$\frac{\partial^\alpha\varphi}{\partial t^\alpha} - \frac{\partial^2\varphi}{\partial x^2} + \varphi^2 = \frac{\Gamma(\frac{5}{2})}{\Gamma(\frac{5}{2}-\alpha)}(1-x)^{\frac{5}{2}}t^{\frac{3}{2}-\alpha} - \frac{15}{4}(1-x)^{\frac{1}{2}}t^{\frac{3}{2}} + (1-x)^5t^3.$$

The analytical solution when $\alpha = 2$, is $\varphi(x,t) = (1-x)^{\frac{5}{2}}t^{\frac{3}{2}}$. The initial and boundary conditions can be extracted from this analytical solution.

Example 4.2. *Consider the following TFNKG equation [18]:*

$$\frac{\partial^\alpha\varphi}{\partial t^\alpha} - \frac{\partial^2\varphi}{\partial x^2} + \varphi + \frac{3}{2}\varphi^3 = \frac{\Gamma(3+\alpha)}{2}\sin(\pi x)t^2 + (1+\pi^2)\sin(\pi x)t^{2+\alpha} + \frac{3}{2}\Big[\sin(\pi x)t^{2+\alpha}\Big]^3.$$

The initial and boundary conditions can be extracted from the analytical solution

$$\varphi(x,t) = \sin(\pi x)t^{2+\alpha}.$$

Examples 4.1 and 4.2 in [18], were solved by Nagy using the SCCM. Also, this author has applied the VIM which is proposed in [17,19] for these problems. In Tables 2–5, we compare our method together with the proposed method given in [18] for the absolute errors between exact and approximate solutions for different values of α at the final time $t = 1$. Given these Tables, it is clear that the presented method is more accurate in comparison with the method given in [18]. The exact and approximate solution $\varphi(x,t)$ in the 3-dimensional graphs are shown in Figures 1 and 3. In Figures 2 and 4, we show the L_2 and L_∞ errors for $\varphi(x,t)$ at different space and time levels.

Table 2. The absolute errors between exact and approximate solutions for different values of α at the final time $t = 1$ for Example 4.1.

x	Method of [18]			Proposed Method		
	$\alpha = 1.5$	$\alpha = 1.7$	$\alpha = 1.9$	$\alpha = 1.5$	$\alpha = 1.7$	$\alpha = 1.9$
0.1	$8.7105e-04$	$6.2045e-04$	$4.3675e-04$	$1.0841e-06$	$1.6188e-05$	$3.2015e-06$
0.2	$6.7781e-04$	$3.1908e-04$	$9.8359e-05$	$2.1356e-06$	$3.5277e-05$	$5.4257e-06$
0.3	$6.2089e-04$	$6.5573e-05$	$4.8897e-04$	$3.1778e-06$	$5.6940e-05$	$3.3276e-05$
0.4	$5.7015e-04$	$1.1160e-04$	$7.6534e-04$	$4.2147e-06$	$7.8251e-05$	$8.6504e-05$
0.5	$5.1476e-04$	$1.9899e-04$	$9.3043e-04$	$5.2283e-06$	$9.4359e-05$	$1.7198e-04$
0.6	$4.8948e-04$	$1.8808e-04$	$9.4248e-04$	$6.1722e-06$	$1.0043e-04$	$2.9944e-04$
0.7	$5.1671e-04$	$6.4274e-05$	$7.5585e-04$	$6.9553e-06$	$9.3563e-05$	$4.7832e-04$
0.8	$5.3919e-04$	$1.2118e-04$	$4.2006e-04$	$7.3934e-06$	$7.3628e-05$	$6.1538e-04$
0.9	$6.0660e-04$	$3.7056e-04$	$5.4848e-05$	$7.0136e-06$	$4.2861e-05$	$4.5176e-04$

Table 3. The absolute errors between exact and approximate solutions for different values of α at the final time $t = 1$ for Example 4.1.

α	(x,t)	VIM [18]	SCCM [18]	Proposed Method
1.4	$(0.1, 0.1)$	$9.2852e-03$	$8.4385e-04$	$2.6303e-05$
	$(0.2, 0.2)$	$2.2201e-02$	$1.1433e-03$	$2.9192e-05$
	$(0.3, 0.3)$	$3.5651e-02$	$5.3780e-04$	$2.7112e-05$
	$(0.4, 0.4)$	$4.9628e-02$	$1.5545e-04$	$2.2942e-05$
	$(0.5, 0.5)$	$6.4449e-02$	$5.3227e-04$	$1.6197e-05$
	$(0.6, 0.6)$	$7.9514e-02$	$1.3268e-03$	$9.4255e-06$
	$(0.7, 0.7)$	$9.1443e-02$	$1.9159e-03$	$5.6314e-06$
	$(0.8, 0.8)$	$8.7942e-02$	$2.0414e-03$	$4.9154e-06$
	$(0.9, 0.9)$	$9.2321e-02$	$1.8996e-03$	$5.5291e-06$
1.6	$(0.1, 0.1)$	$4.1518e-03$	$1.1685e-03$	$6.5452e-05$
	$(0.2, 0.2)$	$1.0319e-02$	$2.5887e-03$	$7.9581e-05$
	$(0.3, 0.3)$	$1.7757e-02$	$2.8863e-03$	$7.5557e-05$
	$(0.4, 0.4)$	$2.6987e-02$	$2.3912e-03$	$6.6870e-05$
	$(0.5, 0.5)$	$3.8327e-02$	$1.7692e-03$	$5.5072e-05$
	$(0.6, 0.6)$	$5.0993e-02$	$1.4174e-03$	$3.4641e-05$
	$(0.7, 0.7)$	$6.1379e-02$	$1.4334e-03$	$7.4212e-06$
	$(0.8, 0.8)$	$5.6577e-02$	$1.6653e-03$	$9.5823e-06$
	$(0.9, 0.9)$	$3.8618e-02$	$1.7449e-03$	$1.1689e-05$

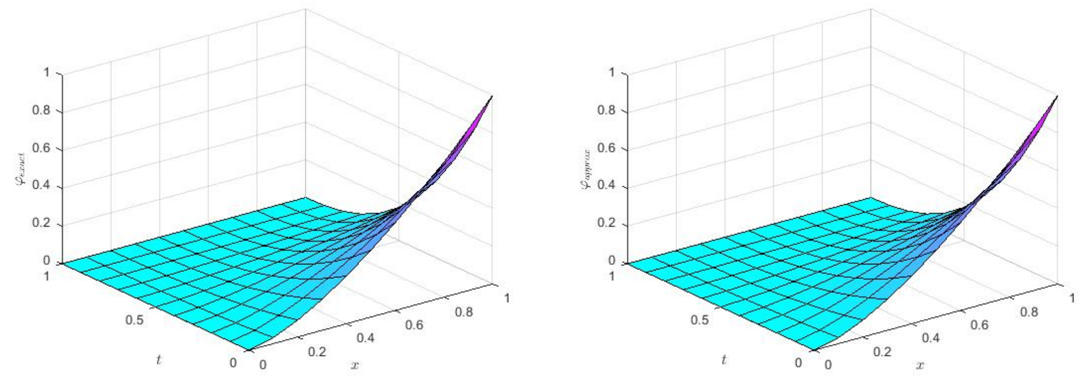

Figure 1. The graphs of the exact solution (left-side) and approximate solution (right-side) for Example 4.1 in case of $\alpha = 1.5$.

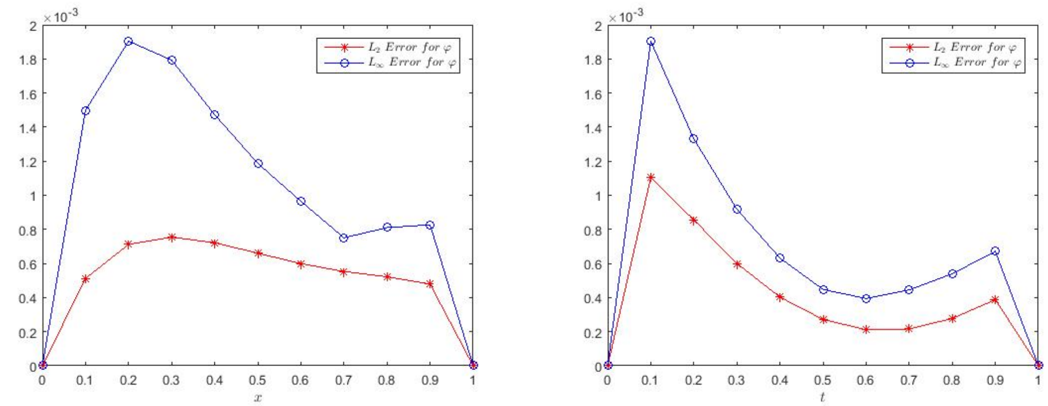

Figure 2. The L_2 and L_∞ errors of Example 4.1 at different space levels (left-side) and time levels (right-side), when $\alpha = 1.5$.

Table 4. The absolute errors between exact and approximate solutions for different values of α at the final time $t = 1$ for Example 4.2.

x	Method of [18]			Proposed Method		
	$\alpha = 1.5$	$\alpha = 1.7$	$\alpha = 1.9$	$\alpha = 1.5$	$\alpha = 1.7$	$\alpha = 1.9$
0.1	$1.6396e-03$	$1.5471e-03$	$1.4380e-03$	$2.5584e-04$	$2.5858e-04$	$1.1890e-05$
0.2	$1.2808e-03$	$1.1272e-03$	$9.4914e-04$	$4.8180e-04$	$4.9042e-04$	$1.9801e-05$
0.3	$1.0869e-03$	$8.9663e-04$	$6.7913e-04$	$6.5495e-04$	$6.7255e-04$	$2.2468e-05$
0.4	$8.4196e-04$	$6.3348e-04$	$3.9687e-04$	$7.6219e-04$	$7.8831e-04$	$2.1890e-05$
0.5	$7.8252e-04$	$5.6868e-04$	$3.2651e-04$	$7.9832e-04$	$8.2794e-04$	$2.1208e-05$
0.6	$8.4196e-04$	$6.3348e-04$	$3.9687e-04$	$7.6219e-04$	$7.8831e-04$	$2.1890e-05$
0.7	$1.0869e-03$	$8.9663e-04$	$6.7913e-04$	$6.5495e-04$	$6.7255e-04$	$2.2468e-05$
0.8	$1.2808e-03$	$1.1272e-03$	$9.4914e-04$	$4.8180e-04$	$4.9042e-04$	$1.9802e-05$
0.9	$1.6396e-03$	$1.5471e-03$	$1.4380e-03$	$2.5584e-04$	$2.5858e-04$	$1.1890e-05$

TABLE 5. The absolute errors between exact and approximate solutions for different values of α at the final time $t = 1$ for Example 4.2.

α	(x,t)	VIM [18]	SCCM [18]	Proposed Method
	$(0.1, 0.1)$	$3.9211e-05$	$2.3809e-05$	$2.8758e-06$
	$(0.2, 0.2)$	$6.1713e-04$	$5.2644e-05$	$2.3338e-05$
	$(0.3, 0.3)$	$2.1989e-03$	$6.0187e-06$	$6.0100e-05$
	$(0.4, 0.4)$	$2.5545e-03$	$6.6640e-05$	$7.2761e-05$
1.4	$(0.5, 0.5)$	$5.3405e-03$	$4.0011e-05$	$5.0678e-06$
	$(0.6, 0.6)$	$3.1409e-02$	$1.5837e-04$	$2.2111e-04$
	$(0.7, 0.7)$	$8.0092e-02$	$9.1922e-04$	$5.4526e-04$
	$(0.8, 0.8)$	$1.3528e-01$	$2.9084e-03$	$8.2187e-04$
	$(0.9, 0.9)$	$1.4272e-01$	$3.8732e-03$	$7.6113e-04$
	$(0.1, 0.1)$	$1.0402e-05$	$2.3809e-05$	$5.7967e-07$
	$(0.2, 0.2)$	$1.4424e-04$	$5.2644e-05$	$5.4262e-06$
	$(0.3, 0.3)$	$6.7151e-05$	$6.0187e-06$	$1.3291e-05$
	$(0.4, 0.4)$	$3.0493e-03$	$6.6640e-05$	$3.9147e-06$
1.6	$(0.5, 0.5)$	$1.6350e-02$	$4.0011e-05$	$6.3841e-05$
	$(0.6, 0.6)$	$4.9599e-02$	$1.5837e-04$	$2.2965e-04$
	$(0.7, 0.7)$	$1.0675e-01$	$9.1922e-04$	$4.8510e-04$
	$(0.8, 0.8)$	$1.6942e-01$	$2.9084e-03$	$7.1863e-04$
	$(0.9, 0.9)$	$1.7521e-01$	$3.8732e-03$	$6.8028e-04$

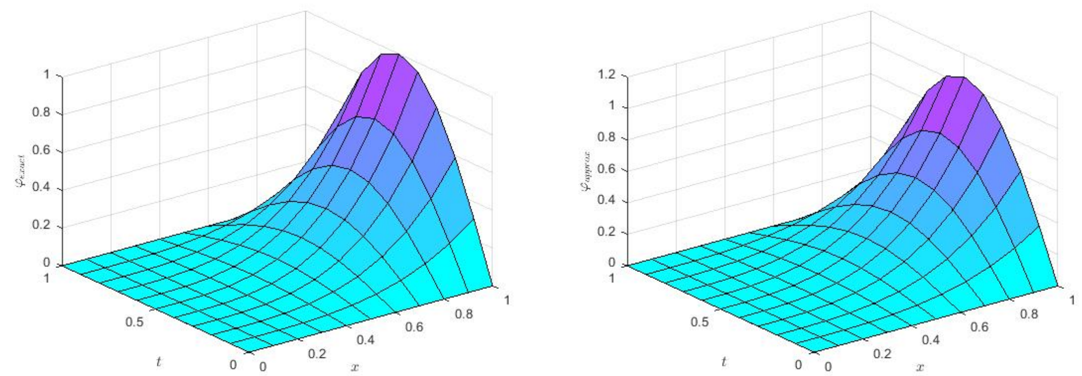

FIGURE 3. The graphs of the exact solution (left-side) and approximate solution (right-side) for Example 4.2 in case of $\alpha = 1.5$.

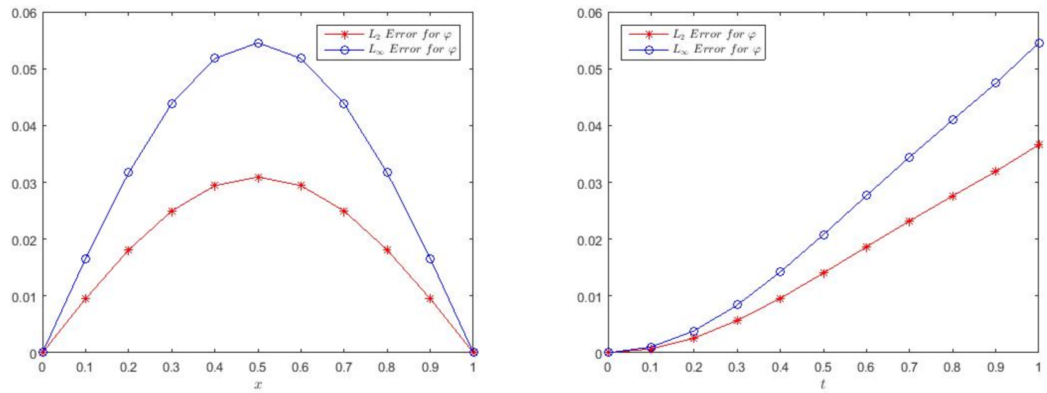

FIGURE 4. The L_2 and L_∞ errors of Example 4.2 at different space levels (left-side) and time levels (right-side), when $\alpha = 1.5$.

5. Conclusion

In this paper, we propose a cubic-Bspline collocation method for obtaining numerical solutions to the TFNKG equation. The TFNKG equation is an extension of the classical KG equation that incorporates fractional derivatives, enabling a more versatile and comprehensive representation of wave phenomena. The cubic-Bspline collocation method is a numerical technique that approximates the solution of the TFNKG equation using cubic B-spline basis functions. This method offers several advantages over traditional numerical methods. It can effectively handle complex initial conditions and boundary conditions, ensuring a wide range of applicability. Additionally, the method exhibits high accuracy in capturing the behavior of the solution and demonstrates computational efficiency, enabling efficient solution computations. To demonstrate the accuracy and applicability of the proposed method, the technique was applied and tested on examples with different nonlinearity terms. The numerical results unequivocally demonstrated that the cubic B-spline collocation method exhibited the highest level of performance among the tested methods. In general, the numerical solutions obtained using the presented method exhibit excellent agreement with the exact solutions. This agreement between the numerical and exact solutions is further supported by the plotted graphs, which validate the reliability and accuracy of the proposed method. As a result, we are confident that the cubic-Bspline collocation method has the potential to become a valuable and versatile tool for effectively solving nonlinear fractional differential equations across various scientific disciplines. Its ability to provide accurate solutions in a wide range of applications makes it a promising approach for researchers and practitioners working in fields such as physics, engineering and applied mathematics.

References

[1] Baleanu, D., Machado, J. A. T. and Luo, A. C., (2011), Fractional dynamics and control, Springer Science & Business Media.

[2] Bambusi, D. and Cuccagna, S., (2011), On dispersion of small energy solutions of the nonlinear Klein–Gordon equation with a potential, American journal of mathematics, 133 (5), pp. 1421–1468.

[3] Bao, W. and Dong, X., (2012), Analysis and comparison of numerical methods for the Klein–Gordon equation in the nonrelativistic limit regime, Numerische Mathematik, 120 (2), pp. 189–229.

[4] Bellman, R. E. and Kalaba, R. E., (1965), Quasilinearization and nonlinear boundary-value problems.

[5] Diethelm, K. and Ford, N. J., (2002), Analysis of fractional differential equations, Journal of Mathematical Analysis and Applications, 265 (2), pp. 229–248.

[6] Prenter, P. M., (2008), Splines and variational methods, Courier Corporation.

[7] Foadian, S., Pourgholi, R. and Hashem Tabasi, S., (2018), Cubic B-spline method for the solution of an inverse parabolic system, Applicable Analysis, 97 (3), pp. 438–465.

[8] Ganji, R., Jafari, H., Kgarose, M. and Mohammadi, A., (2021), Numerical solutions of time-fractional Klein–Gordon equations by clique polynomials, Alexandria Engineering Journal, 60 (5), pp. 4563–4571.

[9] Ghanbari, B., Kumar, S. and Kumar, R., (2020), A study of behaviour for immune and tumor cells in immunogenetic tumour model with non-singular fractional derivative, Chaos, Solitons & Fractals, 133, p. 109619.

[10] Gordon, W., (1926), Der comptoneffekt nach der schrödingerschen theorie, Zeitschrift für Physik, 40 (1-2), pp. 117–133.

[11] Janmohammadi, A., Damirchi, J., Mahmoudi, S. M. and Esfandiari, A., (2022), Numerical solutions of inverse time fractional coupled Burgers' equations by the Chebyshev wavelet method, Journal of Applied Mathematics and Computing, pp. 1–27.

[12] Khader, M., Saad, K. M., Hammouch, Z. and Baleanu, D., (2021), A spectral collocation method for solving fractional Kdv and Kdv-Burgers equations with non-singular kernel derivatives, Applied Numerical Mathematics, 161, pp. 137–146.

[13] Khan, N. A., Riaz, F. and Ara, A., (2016), A note on soliton solutions of Klein–Gordon–Zakharov equation by variational approach, Nonlinear Engineering, 5 (3), pp. 135–139.

[14] Klein, O., (1926), Quantentheorie und fünfdimensionale relativitätstheorie, Zeitschrift für Physik, 37 (12), pp. 895–906.

[15] Kumar, S., Nisar, K. S., Kumar, R., Cattani, C. and Samet, B., (2020), A new rabotnov fractional-exponential function-based fractional derivative for diffusion equation under external force, Mathematical Methods in the Applied Sciences, 43 (7), pp. 4460–4471.

[16] Miller, K. S. and Ross, B., (1993), An introduction to the fractional calculus and fractional differential equations, Wiley, New York.

[17] Molliq, Y., Noorani, M. S. M. and Hashim, I., (2009), Variational iteration method for fractional heat-and wave-like equations, Nonlinear Analysis: Real World Applications, 10 (3), pp. 1854–1869.

[18] Nagy, A., (2017), Numerical solution of time fractional nonlinear Klein–Gordon equation using Sinc–Chebyshev collocation method. Applied Mathematics and Computation 310, pp. 139–148.

[19] Odibat, Z. and Momani, S., (2009), The variational iteration method: an efficient scheme for handling fractional partial differential equations in fluid mechanics, Computers & Mathematics with Applications, 58 (11-12), pp. 2199–2208.

[20] Oldham, K. and Spanier, J., (1974), The fractional calculus theory and applications of differentiation and integration to arbitrary order, Elsevier.

[21] Owolabi, K. M. and Hammouch, Z., (2019), Spatiotemporal patterns in the Belousov–Zhabotinskii reaction systems with Atangana–Baleanu fractional order derivative, Physica A: Statistical Mechanics and its Applications, 523, pp. 1072–1090.

[22] Podlubny, I., (1998), Fractional differential equations: an introduction to fractional derivatives, fractional differential equations, to methods of their solution and some of their applications, Elsevier.

[23] Singh, H., Kumar, D. and Pandey, R. K., (2020), An efficient computational method for the time-space fractional Klein–Gordon equation, Frontiers in Physics, 8, p. 281.

[24] Singh, H., Kumar, D., Singh, J. and Singh, C. S., (2019), A reliable numerical algorithm for the fractional Klein–Gordon equation, Engineering Transactions, 67 (1), pp. 21–34.

[25] Von Rosenberg, D. U., (1969), Methods for the numerical solution of partial differential equations, New York: American Elsevier Publishing Inc.

[26] Wang, K.L., (2023), New perspective on fractional Hamiltonian amplitude equation, Optical and Quantum Electronics, 55 (12), p. 1033.

[27] Wang, K. L. and Wei, C., (2023), Fractal soliton solutions for the fractal-fractional shallow water wave equation arising in ocean engineering, Alexandria Engineering Journal, 65, pp. 859–865.

[28] Wang, K. L., (2023), New solitary wave solutions of the fractional modified Kdv–Kadomtsev–Petviashvili equation, Fractals, 31 (3), p. 2350025.

[29] Wang, K. L., (2023), Solitary wave dynamics of the local fractional Bogoyavlensky–Konopelchenko model, Fractals, 31 (5), p. 2350054.

[30] Wang, K. L., (2023), Investigation of fractional Kdv–Zakharov–Kuznetsov equation arising in plasma physics, Fractals, 31 (7), p. 2350065.

[31] Wang, K. L., (2022), Novel analytical approach to modified fractal gas dynamics model with the variable coefficients, ZAMM - Journal of Applied Mathematics and Mechanics, 103 (6).
[32] Wyss, W., (1986), The fractional diffusion equation. Journal of Mathematical Physics, 27 (11), pp. 2782–2785.

Javad Damirchi is an Assistant Professor of numerical analysis in the Department of Mathematics at Semnan University, Semnan, Iran. He received his B.Sc. and M.Sc. degrees from Iran University of Science & Technology, Iran, in 2002 and 2009 respectively. His major research areas are numerical analysis, numerical solution of ODEs and PDES, Inverse problems of parabolic type, fractional differential equations, and solving mathematical models in engineering and physics.

Saeed Shagholi received his M.Sc. degree from the Department of Engineering Mathematics at Yildiz University in 1991 and his Ph.D. from the Department of Mathematics at Iran University of Science & Technology, Iran, in 2019. He is an assistant professor of geometry and has been working as both research and teaching staff at the Department of Mathematics, Semnan University, Semnan, Iran, since 1991. His research interests include dynamical systems and mathematical models in medicine.

Saedeh Foadian received her B.Sc. degree in applied mathematics (2009), her M.Sc. degree in harmonic analysis (2012), and her Ph.D. degree in 2018 in Applied Mathematics at Damghan University, Iran. Her area of research is the numerical solution of linear and nonlinear partial differential equations.